Contribution of particles and magnetic field lines diffusion to Anomalous transport in tokamak

F.Miskane[1,2], A. Dezairi[1,2], D. Saifaoui[1],H.Imzi[1]
1-Laboratoire de Physique Théorique,
Faculté des sciences Ain Chok, Casablanca, Maroc
2-Laboratoire de Physique Théorique et de La matière Condensée,
Faculté des Sciences Ben M'sik, Casablanca, Maroc

Research into anomalous transport is aimed at two different sources : turbulent fluctuations in either the electric or the magnetic field. In each case a model has been developed describing the influence of fluctuating field on particles transport. The dynamic of particles guiding centers in a configuration of electric and magnetic turbulence is studied in four dimensional equations of motion. An Hamiltonian description shows that the particles trajectories are described by action angle variables system. It has been demonstrated that the island topology appears at positions near resonant surface if there are the small perturbations. Localized chaotic regions appear while increasing the perturbation and spread up to a fully stochastic situation.
The standard definition coefficient D uses the limit of the mean square excursion ; an expression of D useful to describe transport in a finite region can be obtained from the exit times τ_i of particles. In the present paper, we compute the numerical diffusion coefficient in the case of electric and magnetic turbulence, the comparison with quasi-linear theory is made for the two cases. This study indicate that electric fluctuations might be the dominant source of anomalous transport for the particles at low parallel velocity, whereas magnetic fluctuations effect particles transport at great parallel velocity. The D/D_{ql} ratio converge to one for the case where numerical diffusion coefficient coincides well with the quasi-linear diffusion coefficient.

PACS : 52.65.-y Plasma Simulation

I. INTRODUCTION

This work describes the particles behavior in presence of electric and magnetic turbulence. Anomalous transport resulting from fluctuating fields [1,2,3] is considered as the cause of loss of plasma confinement in fusion devices. In this paper, we report results on the transport of particles in considering two different cases: in the first one, the magnetic field is assumed not to be perturbed; enhanced diffusion results electric turbulence which induce transverse drift velocities for the particles guiding centers. In the other case, the diffusion results from the perturbed magnetic field.

The hamiltonian mechanic allows to describe the particles trajectories with action angle variables system. We will see that the main difference between magnetic and electric cases is that the diffusion increases with parallel velocity in the magnetic case, whereas it decreases with the parallel velocity in the electric case.

This paper is organized as follows. In section II we present briefly the equations of particles guiding center and the quasi-linear calculations, section III is devoted to the study of electrostatic turbulence. In section IV, we focus on the magnetic turbulence. A comparison between field lines diffusion and particles diffusion across magnetic surfaces is treated in section V. The numerical results are compared to the quasi-linear prediction and discussed.

II. THE MODEL

A. GUIDING CENTER MOTION

We consider that a plasma in a magnetic field can be represented in the form:
we use here a simplified equilibrium field

$$\mathbf{B}_{eq} = B_\theta \mathbf{e}_\theta + B_0 \mathbf{e}_\varphi \qquad (1)$$

where $B_\theta = \frac{r}{q(r)R_0} B_0$ is the poloidal magnetic field, B_0 is the toroidal field, r the minor radius, θ and φ the poloidal and toroidal angles, and q(r) the safety factor. In the following, we will neglect the field curvature, and the trapping of particles in the local magnetic mirrors.
Since the cyclotron frequency is much larger than the transit and drift frequencies, the motion can be separated in a fast cyclotron gyration and a slow guiding-center motion. The equations of the guiding center motion are :

$$\frac{dx}{dt} = v_{II} \frac{\mathbf{B}}{B} + \frac{\mathbf{B} \wedge \nabla \phi}{B^2} \qquad (2)$$
$$m_i \frac{dv_{II}}{dt} = -e_i \frac{\mathbf{B}}{B} \nabla \phi$$

where m_i , e_i are particle mass and charge.

$$\mathbf{x} \equiv (r, \theta, \varphi)$$

At order 1 in $\frac{r}{R_0}$, this system can be written as :

$$\frac{dr}{dt} = -\frac{1}{Br}\frac{\partial \phi}{\partial \theta}$$
$$\frac{d\theta}{dt} = \frac{v_{II}}{q(r)R_0} + \frac{1}{Br}\frac{\partial \phi}{\partial r} \qquad (3)$$

$$\frac{d\varphi}{dt} = \frac{v_{II}}{R_0}$$
$$\frac{dv_{II}}{dt} = -\frac{e_i}{m_i R_0}\left[\frac{\partial \phi}{\partial \varphi} + \frac{1}{q(r)}\frac{\partial \phi}{\partial \theta}\right]$$

where ϕ is the electric potential perturbation that is given by :

$$\phi(r,\theta,\varphi,t) = \sum_{mn\omega} \tilde{\phi}_{mn\omega}(r)\cos(m\theta - n\varphi - \omega t + \alpha_{mn\omega}) \qquad (4)$$

where $\alpha_{mn\omega}$ are the random phase. We will assume that all perturbations rotate with the same phase velocity $\frac{\omega}{m} = \omega_0$. In this case, there exists a frame where the perturbation is static. The main advantage of this procedure is that the energy $H = \frac{mv_{II}^2}{2} + e\phi$ is invariant in this frame.

In order to simplify our notations, we introduce a reference magnetic surface $r = r_0$ such that $q_0 = \frac{m_0}{n_0}$, where m_0 and n_0 are integers. The summation will be restricted to only one poloidal wave number m_0 and the amplitude are assumed to be radially constant. Also we introduce the helical angle $\alpha = m_0\theta - n_0\varphi$ instead of the poloidal angle θ. The electric potential perturbation becomes with this assumption :

$$\phi(r,\theta,\varphi) = \sum_{p=-L}^{L} \tilde{\phi}_p \cos(\alpha - p\varphi + \alpha_p) \qquad (5)$$

The inverse of the safety factor is expanded as:

$$\frac{1}{q(r)} = \frac{1}{q_0} - \frac{s_0}{q_0}\frac{r - r_0}{r_0} \qquad (6)$$

where $s_0 = \frac{s_0}{q_0}\frac{dq}{dr}\Big|_{r=r_0}$ is the local magnetic shear and $r - r_0$ is the distance from the resonant rational surface. we introduce the further normalisation

$$\tau = \frac{v_{T_s}}{R_0}t \ , \ \xi = \frac{v_{II}}{v_{T_s}}, \ x = \frac{r - r_0}{w} \ , \ \phi_p = \frac{e_i\tilde{\phi}_p}{2T_s} \qquad (7)$$

consequently, the system then becomes :

$$\frac{dx}{d\tau} = \sum_{p=-L}^{L} \phi_p \sin(\alpha - p\varphi + \alpha_p)$$
$$\frac{d\alpha}{d\tau} = x\xi - \Omega \qquad (8)$$

$$\frac{d\varphi}{d\tau} = \xi$$
$$\frac{d\xi}{d\tau} = \sum_{p=-L}^{L} (x - p)\phi_p \sin(\alpha - p\varphi + \alpha_p)$$

where we have chosen $\frac{m_0\rho_s}{r_0}\frac{R_0}{w} = 1$ (ρ_s is the Larmor radius) $\rho_s = \frac{m_i v_{T_s}}{eB_0}$ and $\Omega = m_0\frac{\omega_0 R_0}{v_{T_s}}$. T_s is a temperature, $v_{T_s} = (\frac{2T_s}{m_i})^{1/2}$ a thermal velocity, $\omega = -\frac{q_0 r_0}{m_0 s_0}$ is a distance between resonant surfaces.

B. HAMILTONIAN DESCRIPTION

An Hamiltonian description of charged particles dynamic prove a strong tool, the charged particles trajectories are described by action-angle variables system. The question of particles diffusion in tokamak may be taken up with developed techniques by study of Hamiltonian chaos. In fact, the charged particle motion is Hamiltonian.
It is then convenient to introduce the action variables :

$$I = \xi - \frac{x^2}{2} \quad \text{and} \quad J = x \qquad (9)$$

the system above is an Hamiltonian system , it can be written as

$$\frac{d\alpha}{d\tau} = \frac{\partial H}{\partial J} \qquad \frac{dJ}{d\tau} = -\frac{\partial H}{\partial \alpha} \qquad (10)$$

$$\frac{d\varphi}{d\tau} = \frac{\partial H}{\partial I} \qquad \frac{dI}{d\tau} = -\frac{\partial H}{\partial \varphi}$$

where $H = H_{eq}(I,J) + \sum_p \phi_p \cos(\alpha - p\varphi + \alpha_p)$

and $H_{eq}(I,J) = \frac{\xi^2}{2} - \Omega x = \frac{1}{2}(I + \frac{J^2}{2})^2 - \Omega J \qquad (11)$

H_{eq} is the unperturbed Hamiltonian. For a passing particle, the angle variable are the poloidal and toroidal angle θ and φ.

The associated Hamiltonian is $H = \frac{m_i v_{II}^2}{2} + e_i\phi$.

It can be verified that the system (2) is equivalent to Hamiltonian equations with this set of variables. It can be also verified by replacing the angle θ with the angle α,

the action M is changed into I, with the appropriate normalisation. The frequencies associated with the equilibrium Hamiltonian are :

$$\omega_I = \frac{\partial H_{eq}}{\partial I}\Big]_J = I + \frac{J^2}{2} = \xi(I,J) \qquad (12)$$

$$\omega_J = \frac{\partial H_{eq}}{\partial J}\Big]_I = (I + \frac{J_2}{2})J - \Omega = \xi(I,J)x - \Omega$$

Therefore, the resonance condition for one perturbation is

$$\omega_J - p\omega_I = \xi(x-p) - \Omega = 0 \qquad (13)$$

This condition is strictly equivalent to the Landau resonance condition $\omega - k_{II} v_{II} = 0$. In the limit of large velocities or for zero frequency, the resonance is localized on resonant surfaces x= p.

We consider resonant initial conditions which satisfy the condition (13) $x_0 \xi_0 = \Omega$. Developing the Hamiltonian (11), one finds that the trajectories describe an island topology in the phase space.

$$K = \frac{1}{2} C \tilde{J}^2 + \phi_0 \cos\alpha \qquad (14)$$

where we have chosen $\alpha_0 = 0$, and

$$C = \frac{\partial^2 H_{eq}}{\partial J^2}\Big]_{I_0, J_0} = I_0 + \frac{3}{2} J_0^2 = \xi_0 + x_0^2 \qquad (15)$$

Using the resonance condition (13) for p=0, the curvature C can also be written as $C = \frac{\Omega}{x_0} + x_0^2$. The motion in (α, J) is described by the equation

$$\frac{\partial \alpha}{\partial \tau} = \frac{\partial K}{\partial J} \qquad \frac{\partial \tilde{J}}{\partial \tau} = -\frac{\partial K}{\partial \alpha} \qquad (16)$$

whereas the angle φ is solution of the equation.

$$\frac{d\varphi}{d\tau} = \xi \cong x_0 \tilde{J} \qquad (17)$$

For small perturbations, the width of this island is $W_J = 2(\frac{\phi_0}{C})^{1/2}$. We will call it electrostatic island by analogy with a magnetic island .The island shape is then essentially in the real space i.e.

$$K = \frac{1}{2} \xi_0 \tilde{x}^2 + \phi_0 \cos\alpha \qquad (18)$$

this situation close to a magnetic island .

In the opposite case where the initial velocity is close to zero, $\xi_0 \pi\pi x_0^2$, the position of the particle is almost constant and the particle is trapped along field lines. By trapping we mean that the velocity $\xi(t)$ reverses it sign periodically, similar to the bounce motion of particles trapped in the minimum of a tokamak magnetic field. For small deviations $\tilde{x}$, the bounce motion is described by the island equation:

$$K = \frac{1}{2} x_0^2 \tilde{x}^2 + \phi_0 \cos\alpha \qquad (19)$$

The minimum of potential correspond to $\alpha = \pi$. The condition for trapping along the field line is that the velocity ξ_0 at $\alpha_0 = \pi$ verifies the constraint

$\xi_0 \, p \, 2[\phi_0]^{1/2}$. The bounce angle is then determined by the equation $2\cos(\alpha_0/2) = \frac{\xi_0}{2[\phi_0]^{1/2}}$

C. PARTICLES DIFFUSION

The diffusion coefficient is evaluated in studying the particle response to perturbations. We can study this response by the investigation of evolution of particle distribution function F(**J** ,t), where **J** is the vector (I, J).

F(**J**, t) verify the Vlasov equation

$$\frac{\partial F}{\partial t} + [F, H] = 0 \qquad (20)$$

with F and H are represented by the Fourier decomposition:

$$H = H_{eq}(J) + \sum_{n\omega} h_{n\omega} \exp i(n\Phi - \omega t) \qquad (21)$$

$$F = F_{eq}(J) + \sum_{n\omega} f_{n\omega} \exp i(n\Phi - \omega t)$$

where Φ is the vector (α, φ)

The mean on angular variables of Vlasov equation gives the flux term

$$\Gamma = \sum_n h_{-n}(\inf_n) \qquad (22)$$

The linearisation of Vlasov equation gives the relations:

$$\frac{\partial F_{eq}}{\partial t} = \frac{\partial}{\partial J_k}(D_{ql} \frac{\partial}{\partial J_l} F_{eq}) \qquad (23)$$

$$\text{with } Dql = \pi \sum_{n\omega} |h_n|^2 n_l n_k \delta(\sum_l n_l \frac{\partial H_{eq}}{\partial J_k} - \omega) \qquad (24)$$

in the radial direction D_{ql} becomes

$$D_{ql} = \frac{\pi}{2}\frac{(\phi_0)^2}{|\xi_0|} \qquad (25)$$

The island width is close to

$$W_J = 2\left(\frac{\phi_0}{\xi_0}\right)^{1/2} \qquad (26)$$

III. ELECTROSTATIC TURBULENCE

A. PARTICLES TRAJECTORIES

The trajectories described by the system (8) are computed with a fourth order Runge-Kutta numerical scheme. The time step is determined in order to maintain a constant energy for each particle with a good accuracy. The island topology as described by Eq.(14) has been verified for the case of a single perturbation, as well as the time invariance of the action variable $I = \xi - \frac{x^2}{2}$. All the case in the following are such that $\Omega = 0$, and all the phases $\alpha_p = 0$, In this particular case, the potential is given by the relation

$$\phi = \phi_0 \cos(\alpha)\frac{\sin\left[(2L+1)\frac{\varphi}{2}\right]}{\sin\frac{\varphi}{2}} \qquad (27)$$

Particle trajectories are followed with a Poincaré map corresponding to ''poloidal''plane, i.e. by plotting the position (r,α) of each particle when it crosses the plane $\varphi = 0 \ [\mathrm{mod}\ 2\pi]$.The fig-1 shows Poincaré maps of N=40 particles, which is an initial energy $E_0 = 4$, for 6 values of potential ϕ_0. The number of perturbations is 3 (L=1). The first case is still integrable : 3 islands appear, localized on the resonant surfaces x=-1,0 and 1.Localized chaotic regions appear for $\phi_0 = 0{,}1$ and spread up to a fully stochastic situations $(\phi_0 = 0.8)$. The critical threshold is determined in the following manner : particles are launched at $x_0 = 0$, $\varphi_0 = 0$ with initial α_0 equally distributed over the interval $[0,\pi]$ (this restriction is allowed since with zero phases α_p, the system is symmetric when changing α in $-\alpha$). When one particle reaches the edge of the box, it is considered that the last KAM surface is broken. We found that the onset of global stochasticity agrees rather well with the S=2/3 criterion.

The case with many perturbations is a problem of Hamiltonian chaos [4]. To evaluate the transition to chaos, we apply the 2/3 rule, i.e. when we have the condition $\frac{\phi_0}{\xi_0}\,\phi\,\frac{1}{9}$ that is in good agreement with our results.

The fig.2 shows Poincaré of N=100 particles, with an initial energy E_0=8, for 3 values of parallel velocity ξ_0, The number of perturbations is 3 (L=1). We can observe the trapping phenomena in the low velocity domain. It is shown that an inward pinch occurs whenever cold particles (by cold we mean particles with a velocity smaller than the thermal velocity) diffuse faster than hot particles

B. DIFFUSION COEFFICIENT

In the case where the Chirikov parameter is above the critical value, the particles are expected to exhibit a random motion. We will compute here two effective ''diffusion'' coefficient. The first one is determined from the ratio $\left\langle (x - \langle x\rangle^2)\right\rangle / 2t$, whereas the second is determined by computing an average exit time. It is indeed well known that for particles launched in the interval $[-\delta d, \delta d]$ in the radial (x), the diffusion coefficient is given by therelation :

$$D_J = \frac{1}{\beta(2)+\beta(4)\delta^2+\beta(6)\delta^4}\frac{d^2}{4}\lim_{N\to\infty}\frac{1}{N}\sum_{i=1}^{N}\frac{1}{\tau_i} \qquad (28)$$

where $\beta(2) = \sum_{k=0}^{+\infty}\frac{(-1)^k}{(1+2k)^{2p}}$

and $\beta(4) = \beta(6) = 0$

We find a good agreement between the two methods. The fig-3 shows quasi-linear and numerical diffusion coefficient as function of the perturbation amplitude ϕ_0 for several parallel initial velocities ξ_0 . this figure show that the computed diffusion coefficient agrees with the quasi-linear prediction. We can observe that at low velocity, the diffusion coefficient is lower than the quasi-linear value, this can be explained by the fact that many particles at low velocity are trapped in the potential minima and leave the domain in a very short time scale, with a non diffusive motion. The fig-4 shows the same data as function of ξ_0 for different values of the potential. In this figure, we can observes that the diffusion coefficient decreases with the initial velocities.

The case at large velocity is close to the classical problem of particle trajectories in presence of magnetic islands [1,6-9,10]. At low initial velocities, our results show that the behavior with velocity is less divergent than the $1/\xi_0$ dependence predicted by the quasi-linear theory. In fig-5, we represent the D/D_{ql} ratio as

function of the perturbation amplitude ϕ_0 for several initial velocities ξ_0 according to Mendoça model. the D / D_{ql} ratio converges to one for the case where numerical diffusion coefficient coincides well with the quasi-linear diffusion coefficient.

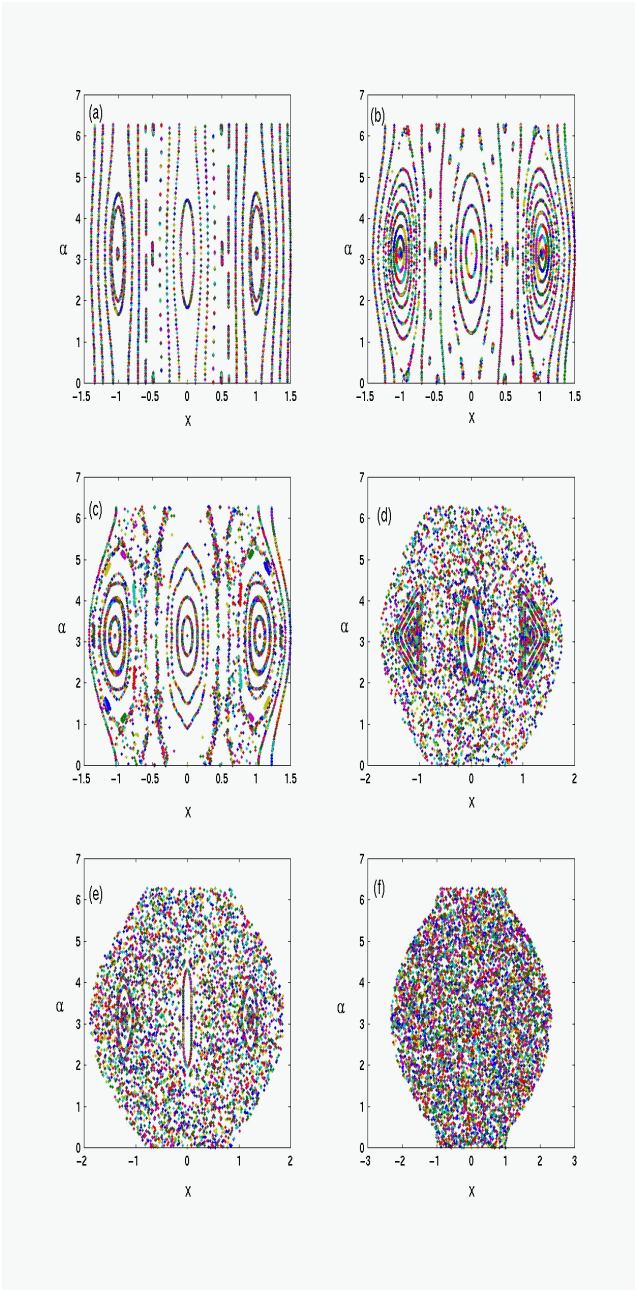

FIG. 1. Poincaré maps of 40 particles, with a initial energy $E_0 = 4$, for 6 values of the potential ϕ_0. (a) $\phi_0 = 0.02$, (b) $\phi_0 = 0.06$, (c) $\phi_0 = 0.1$, (d) $\phi_0 = 0.3$, (e) $\phi_0 = 0.4$, and (d) $\phi_0 = 0.8$. The number of perturbations is 3 (L=1)

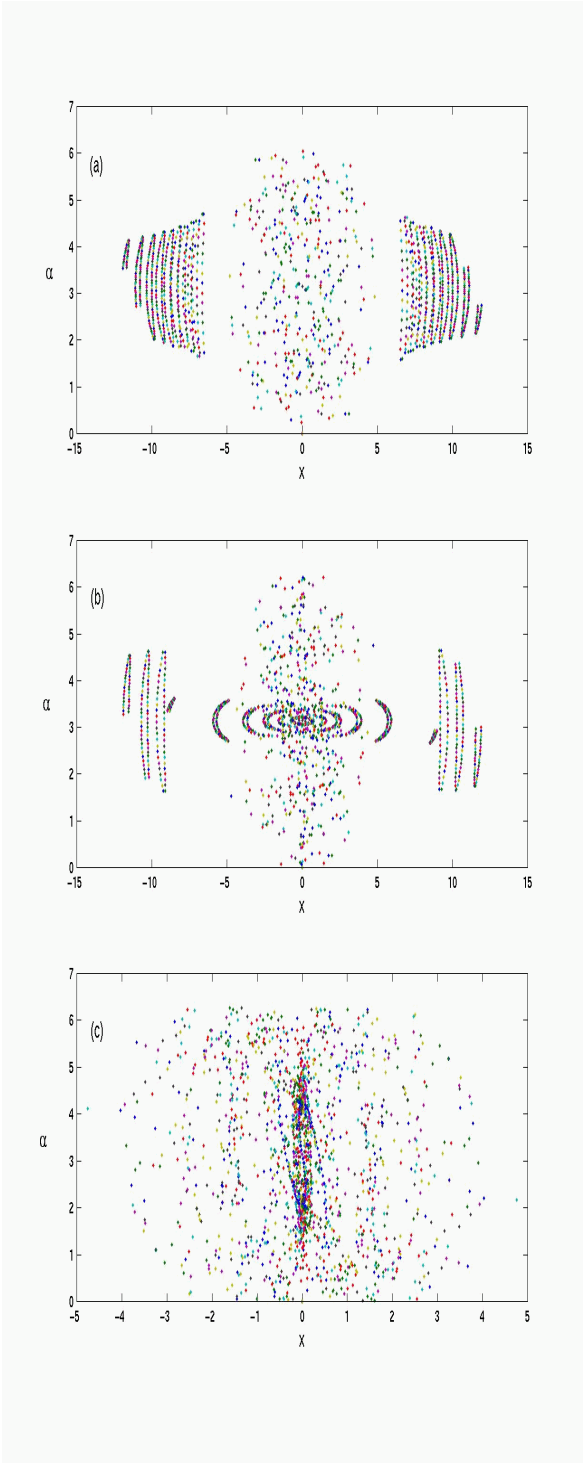

FIG. 2. Poincaré maps of N=100 particles, with a initial energy E_0=8, for 3 values of parallel velocity ξ_0, (a) $\xi_0 = 0.02$, (b) $\xi_0 = 0.5$, and (c) $\xi_0 = 3$. The number of perturbations is 3 (L=1).

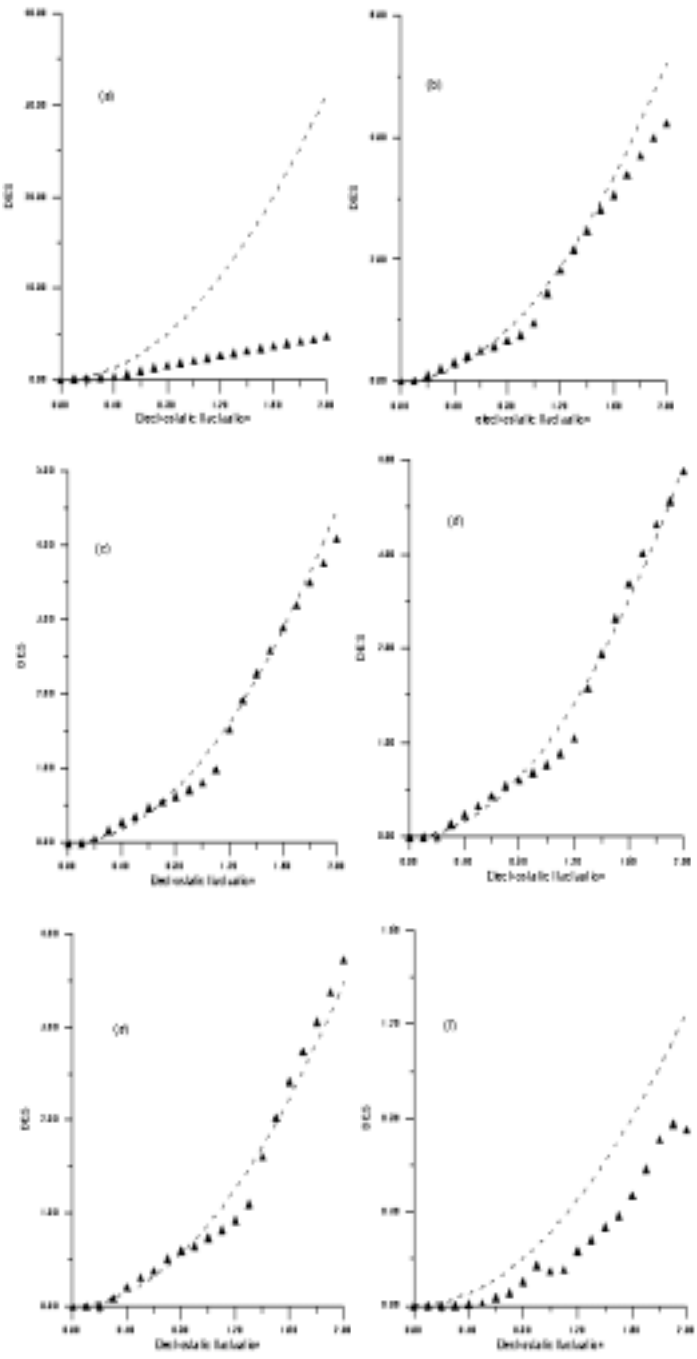

FIG. 3. Electrostatic Diffusion coefficient DES calculated from the particle exit times as function of the perturbation amplitude ϕ_0 for six initial velocities ξ_0 : a) $\xi_0 = 0.2$; b) $\xi_0 = 1.2$; c) $\xi_0 = 1.4$; d) $\xi_0 = 1.6$; e) $\xi_0 = 1.8$ and f) $\xi_0 = 5$---- indicate the quasi-linear prediction and ▲▲▲▲ indicate the computed diffusion coefficients.

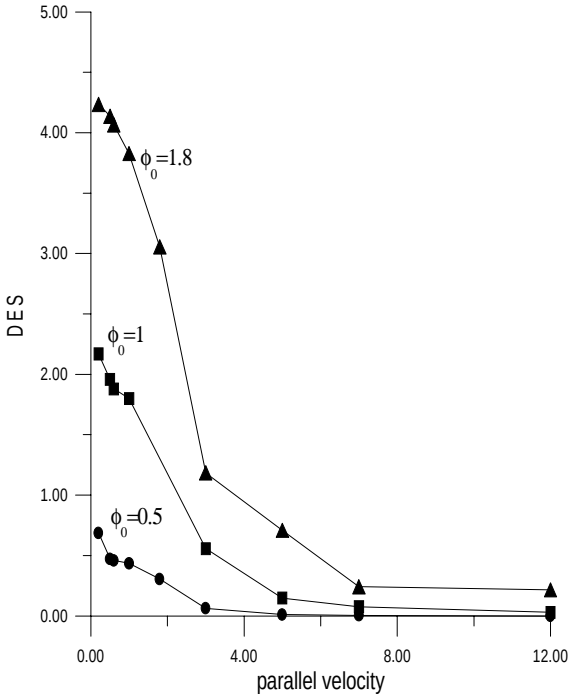

FIG. 4. Electrostatic Diffusion coefficient DES calculated as function of the initial velocities ξ_0 for three values of the perturbation amplitude ϕ_0 : $\phi_0 = 1.8$, $\phi_0 = 1$, $\phi_0 = 0.5$

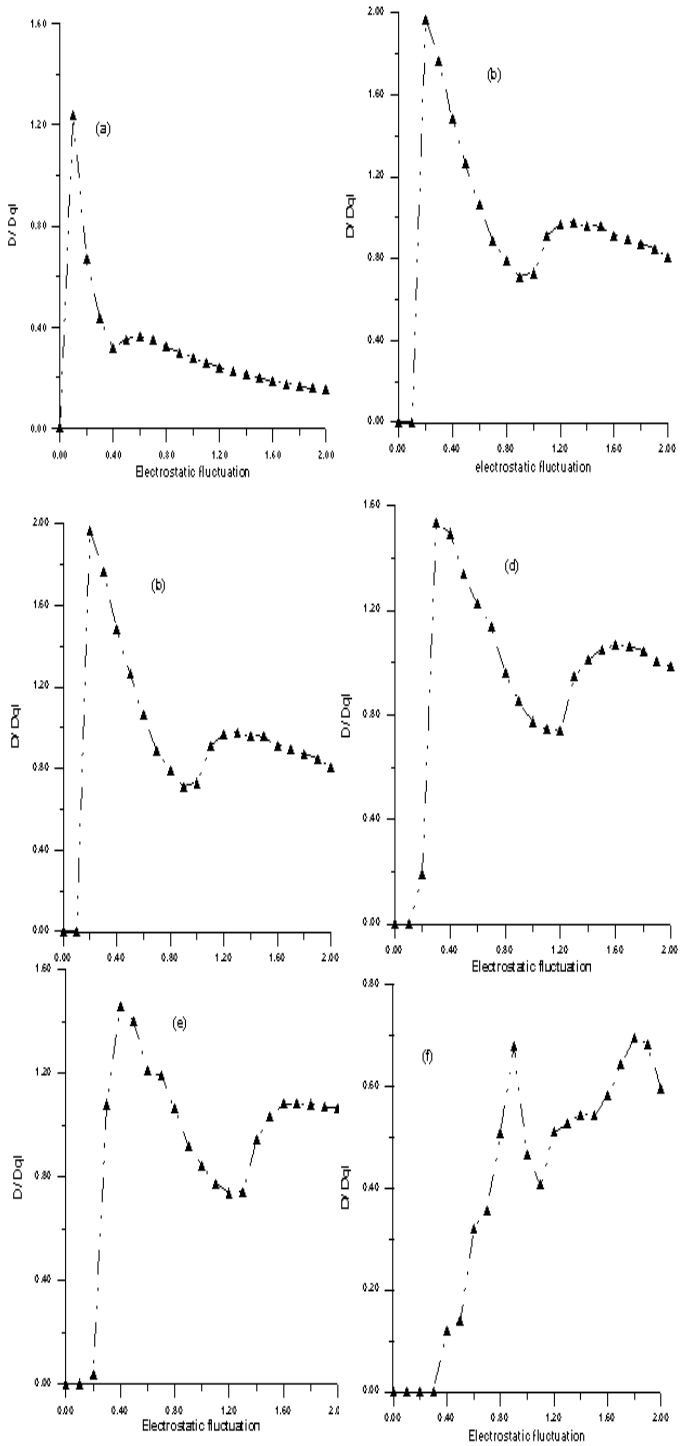

FIG. 5. : The ratio D / D_{ql} calculated numerically as function of the electrostatic perturbation amplitude ϕ_0 for six initial velocities ξ_0 :
(a) $\xi_0 = 0.2$, (b) $\xi_0 = 1.2$, (c) $\xi_0 = 1.4$ (d) $\xi_0 = 1.6$, (e) $\xi_0 = 1.8$ and (f) $\xi_0 = 5$

IV. MAGNETIC TURBULENCE:

A. EQUATIONS OF MOTION

If we consider a plasma in a magnetic field that it can be represented in the form

$$\mathbf{B}=\mathbf{B}_{eq}+\tilde{\mathbf{B}} \tag{29}$$

where $\tilde{\mathbf{B}} = \nabla \wedge \tilde{\mathbf{A}}$ is the fluctuating part and $\tilde{A}$ is the fluctuating vector potential

$\tilde{A}$ can be represented by a Fourier decomposition

$$\tilde{A}(r,\theta,\varphi) = \sum_{p=-L}^{L} \tilde{A}_p \cos(\alpha - p\varphi + \alpha_p) \tag{30}$$

where we impose the amplitude $\tilde{A}_p$ constant for all perturbations.

We have obtained nearly the same results, but the difference between the electrostatic case is that the parallel velocity is still constant. The differential system for it is then:

$$\frac{dx}{dt} = \sum_{p=-L}^{L} -v_{T_s}\xi A_p \sin(\alpha - p\varphi + \alpha_p)$$

$$\frac{d\alpha}{dt} = x\xi - \Omega \qquad \frac{d\varphi}{dt} = \xi \tag{31}$$

where $A_p = \dfrac{e_i \tilde{A}_p}{2T_s}$

this result has been already obtained by Sabot[11]. The Hamiltonian for magnetic perturbation is then where

$$H = H_{eq}(I,J) + \sum_p (-v_{T_s}\xi_{eq} A_p)\cos(\alpha - p\varphi + \alpha_p) \tag{32}$$

with $H_{eq}(I,J) = \dfrac{\xi_{eq}}{2} - \Omega x = \dfrac{1}{2}(I + \dfrac{J^2}{2})^2 - \Omega J$

is the unperturbed Hamiltonian

$$\xi = \xi_{eq} + \tilde{\xi}$$

and $$\tilde{\xi} = \sum_p v_{T_s} A_p \cos(\alpha - p\varphi + \alpha_p)$$

For one perturbation, the calculation of Hamiltonian involves that the trajectories describe a magnetic island topology in the phase space.

$$K = \frac{1}{2}C\tilde{J}^2 + h_0 \cos\alpha \tag{33}$$

where $C = \left.\dfrac{\partial^2 H_{eq}}{\partial J^2}\right]_{I_0,J_0} = I_0 + \dfrac{3}{2}J_0^2 = \xi_{eq,0} + x_0^2$

The width of magnetic island is then

$$W_J = 4\left(\frac{-v_{T_s}\xi_{eq,0}A_0}{\xi_{eq,0} + x_0^2}\right)^{1/2} \tag{34}$$

B. DIFFUSION COEFFICIENT

For the calculation the diffusion coefficient, we proceeded the same that in the electrostatic case. The usual assumption about the transport due to magnetic turbulence was that many modes are present and that the turbulence is well developed, and therefore that the quasi-linear theory was applicable [1].We compute the diffusion coefficient for different values of magnetic

perturbation amplitude with 100 initial conditions and we have considered three interacting islands. The evolution is the same as the electrostatic case, i.e., the diffusion increases with the perturbation, this is shown in fig-6 for six values of numerical diffusion coefficient compared to D_{ql} .As expected, the agreement is fairly good. the diffusion increases with parallel velocities (see fig-7) contrarily to the electrostatic case where the diffusion decreases with parallel velocities. This result is in agreement with the quasi-linear theory . The ratio D / D_{ql} is plotted for several perturbation amplitudes(see fig-8).

V. COMPARISON BETWEEN FIELD LINES DIFFUSION AND PARTICLES DIFFUSION ACROSS MAGNETIC SURFACES

The evolution of stochastic magnetic field lines has been already studied numerically [11]. We have developped a numerical technique in order to study the transition from partial stochasticity to global stochasticity of magnetic field lines. We also introduced a model of diffusion coefficient in order to study the diffusion of lines through magnetic surfaces. The non-Gaussian dynamics of lines has been analyzed using the Kurtosis parameter. Laval [12] has given the particles diffusion coefficient D_p and Field lines diffusion coefficient D_L according to relation $D_L = vD_p$ where v is the particle constant velocity along the field lines. So the field lines diffuse across the plasma and the particle motion along these field lines gives rise to the anomalous diffusion.

A. EQUATION OF FIELD LINES AND DISCETE MAPPING

The magnetic field lines may be transformed in mapping structure .Their general form is found in [8]:

$$I_{k+1} = I_k + \sum_m K_m \sin(m\theta_k) \qquad (35)$$

$$\theta_{k+1} = \theta_k + I_{k+1}$$

where $I_k = 2\pi\psi_k$, $K_m = (2\pi)^2 m f_m$ (36)

For $m = 1$, we find the standard mapping
The generalized mapping that we have used in this work correspond to $m = 2$ writes as

$$I_{k+1} = I_k + K_1 \sin(\theta_k) + K_2 \sin(2\theta_k) \qquad (37)$$

$$\theta_{k+1} = \theta_k + I_{k+1}$$

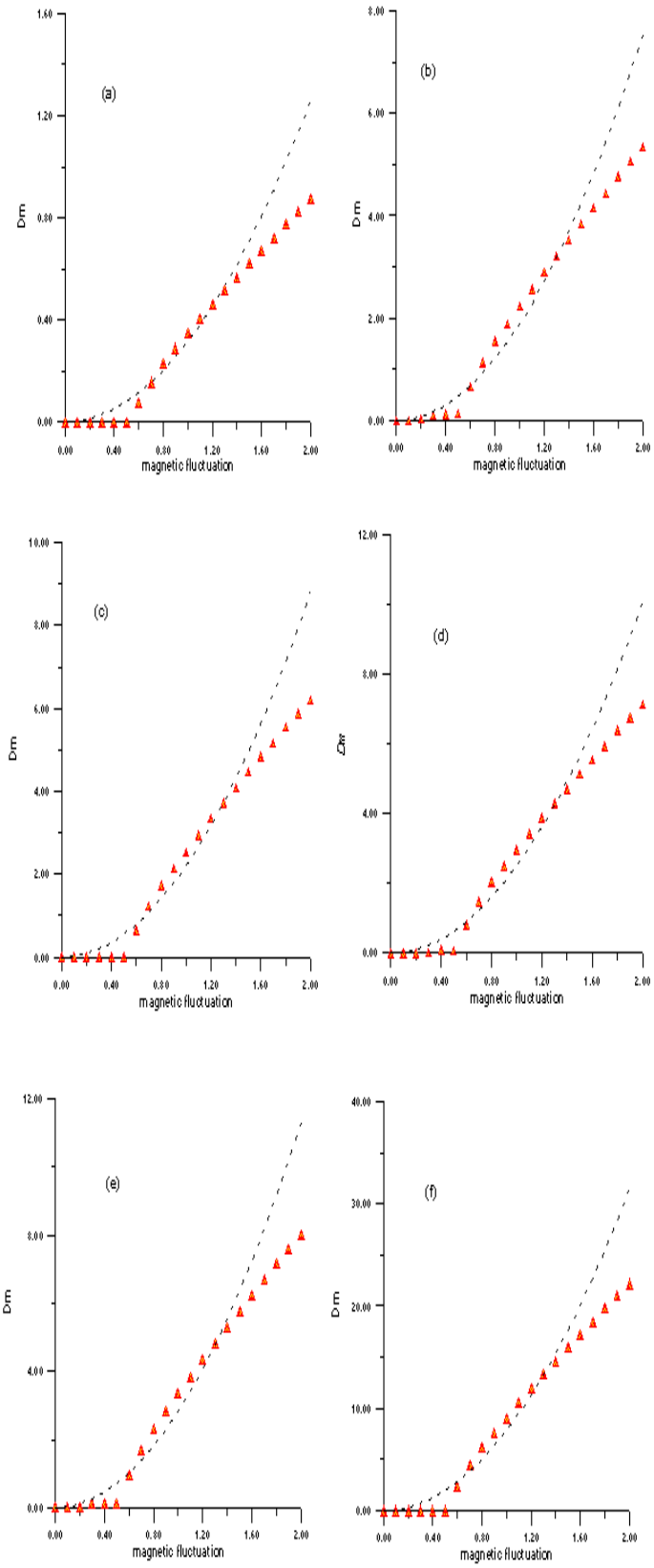

FIG. 6. Magnetic Diffusion coefficient calculated from the particle exit times as function of the perturbation amplitude ϕ_0 for six initial velocities ξ_0 : $\xi_0 = 0.2$, $\xi_0 = 1.2$ $\xi_0 = 1.4$, $\xi_0 = 1.6$, $\xi_0 = 1.8$ and $\xi_0 = 5$

- - - - indicate the quasi-linear prediction

▲ ▲ ▲ ▲ indicate the computed diffusion coefficient

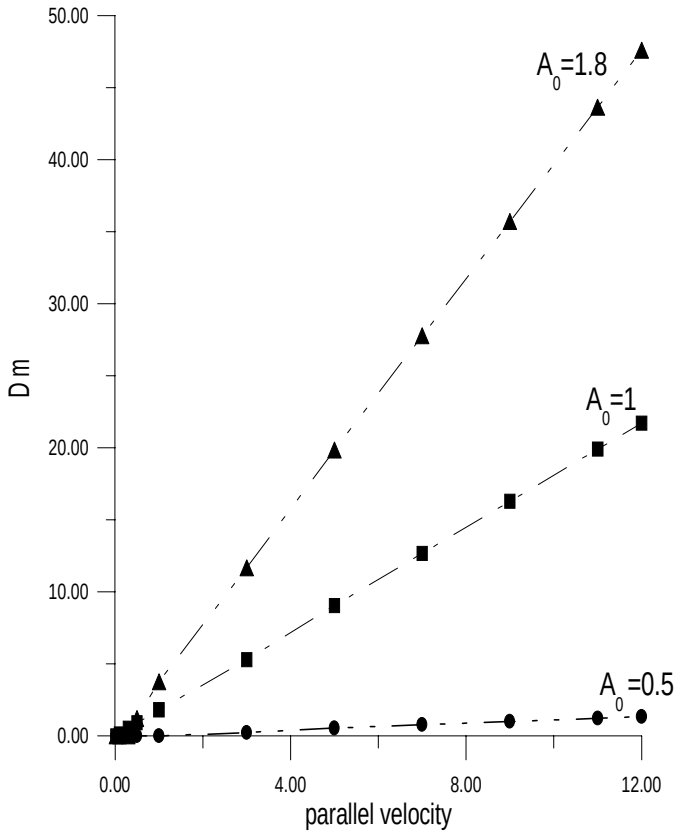

FIG. 7. Magnetic Diffusion coefficient Dm calculated as function of the initial velocities ξ_0 for three values of the perturbation amplitude ϕ_0 : $\phi_0 = 1.8$, $\phi_0 = 1$, $\phi_0 = 0.5$

B. THE POINCARÉ SECTION OF MAGNETIC FIELD LINES - SIMULATIONS

To study the stochastic magnetic field lines we have represented the Poincaré section described by the generalized mapping Equations. (35) in the (ψ,θ) and (x,y) for different values of (K_1, K_2). In the Figures (8-12) the Poincaré section is represented in (ψ,θ) plan, whereas Figures (13-16) are in the (x,y) plan with $x = \psi\cos\theta$ and $y = \psi\sin\theta$.

Figures 8,9,13 and 14 correspond to the case of weak islands overlaping (partial stochasticity). There exist many integrable trajectory (KAM tori) separating different stochastic regions. On the other hand, in plots V 10,11 and 14,15 the islands are large enough to overlap (global stochasticity). The stochastic regions cover all space (there are no KAM tori). We note also that in this case ($K_2 \neq 0$) the last KAM tori is destroyed for values of K_1 different to K_c (K_c =0.97 is the Chirikov constant). The transition points (K_1,K_2) from partial to global stochasticity have been calculated numerically in [4].

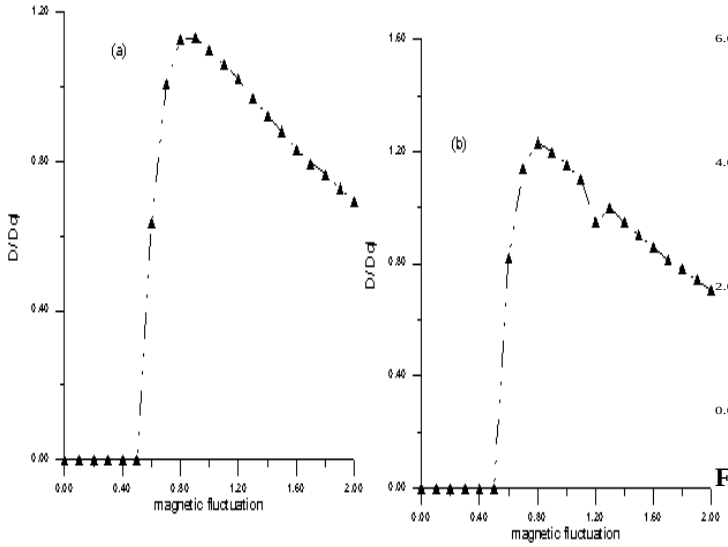

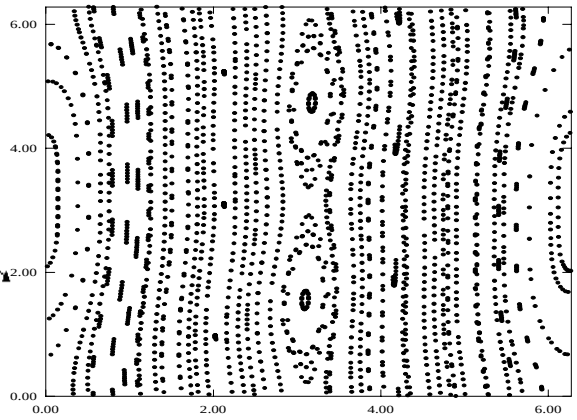

FIG.8 . Poincaré section of the magnetic field lines for $(K_1, K_2) = (0.08, 0.04)$

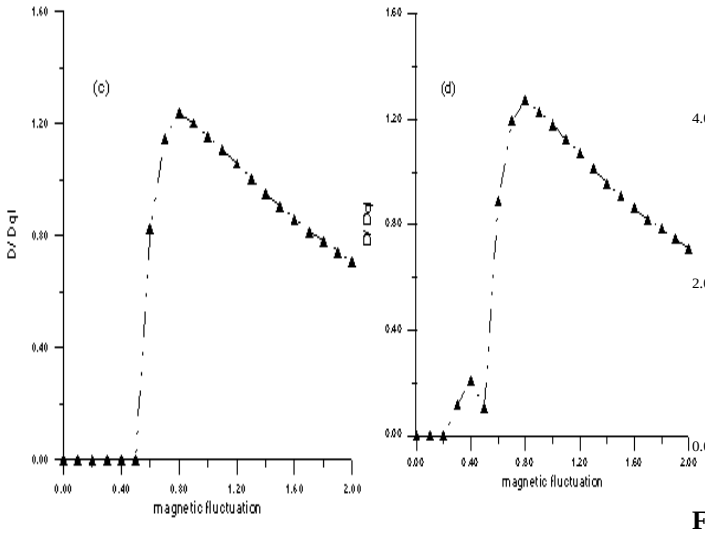

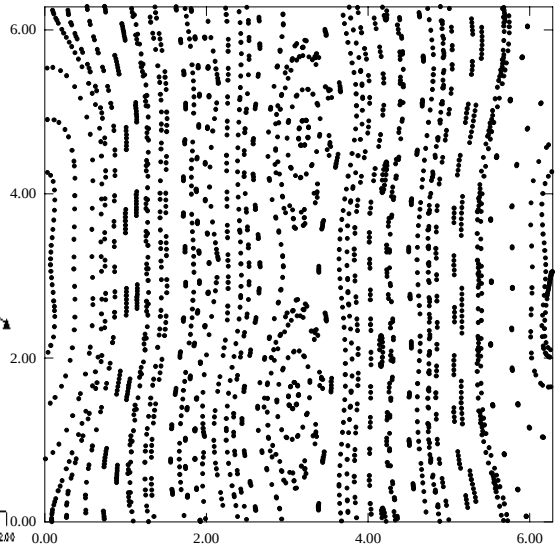

FIG. 9 . Poincaré section of the magnetic field lines for $(K_1, K_2) = (0.12, 0.08)$

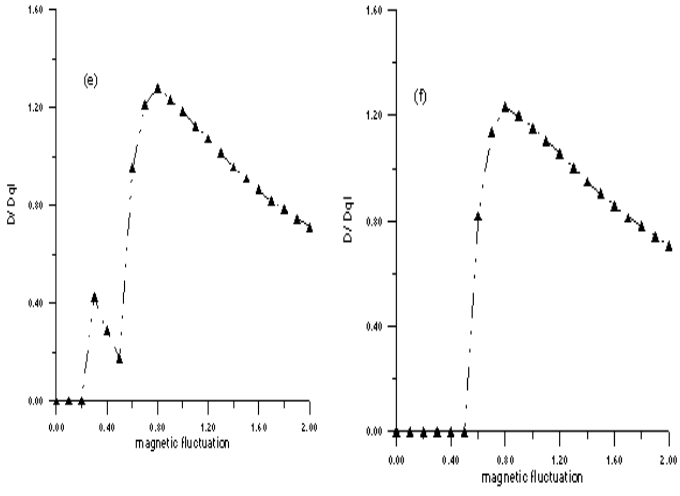

FIG. 8. The ratio D / D_{ql} calculated numerically as function of the magnetic perturbation amplitude φ_0 for six initial velocities ξ_0 : (a) $\xi_0 = 0.2$ (b) $\xi_0 = 1.2$ (c) $\xi_0 = 1.4$ (d) $\xi_0 = 1.6$ (e) $\xi_0 = 1.8$ and (f) $\xi_0 = 5$

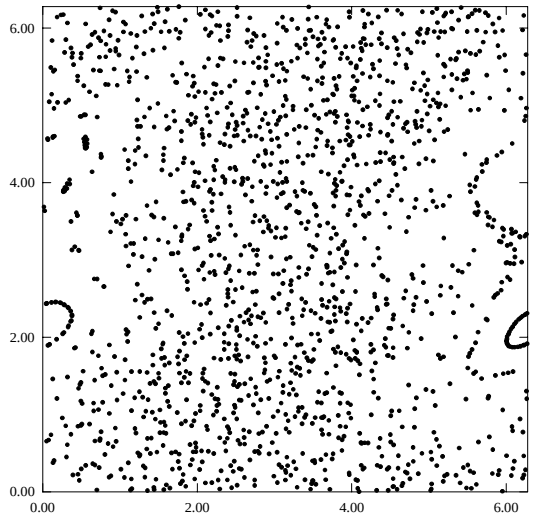

FIG.10. Poincaré section of the magnetic field lines for $(K_1, K_2) = (0.9, 0.9)$

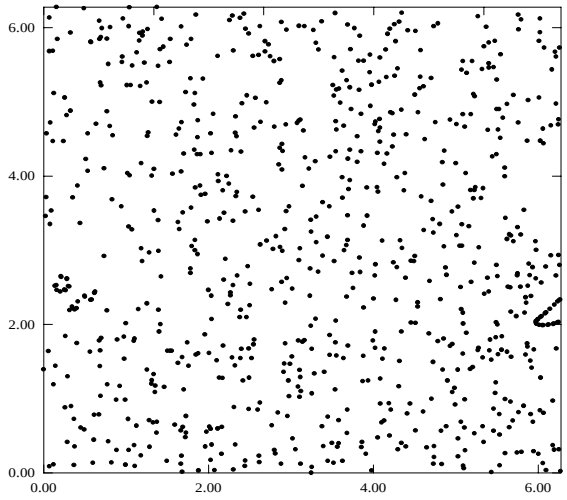

FIG. 11 .Poincaré section of the magnetic field lines for $(K_1, K_2) = (1.8, 1.6)$

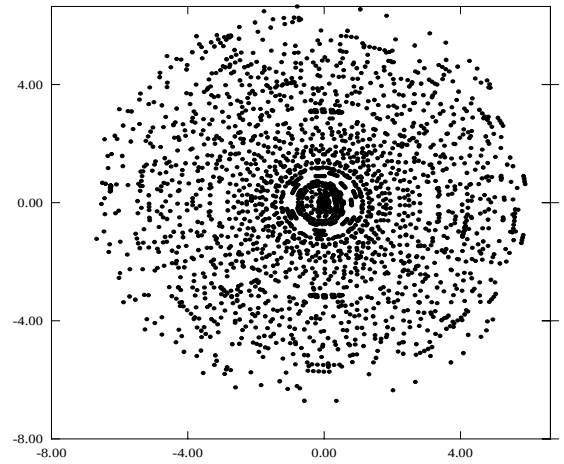

FIG.12.- The evolution of stochastic magnetic field lines in the plane

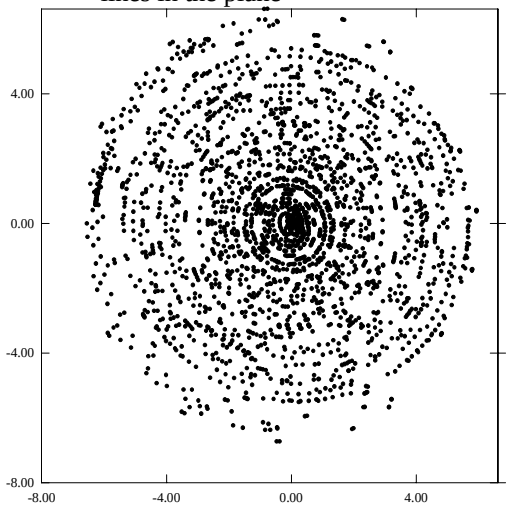

FIG.13. The evolution of stochastic magnetic field lines in the plane (x, y) for valu (K_1, K_2)= (0.12,0.08).

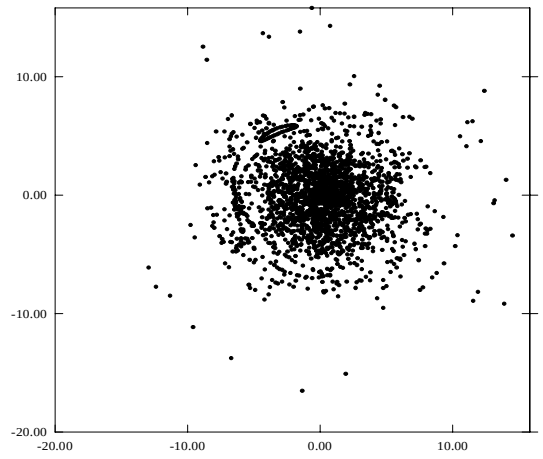

FIG. 14.- The evolution of stochastic magnetic field lines in the plane (x, y) for values of (K_1, K_2)= (0.9,0.9).

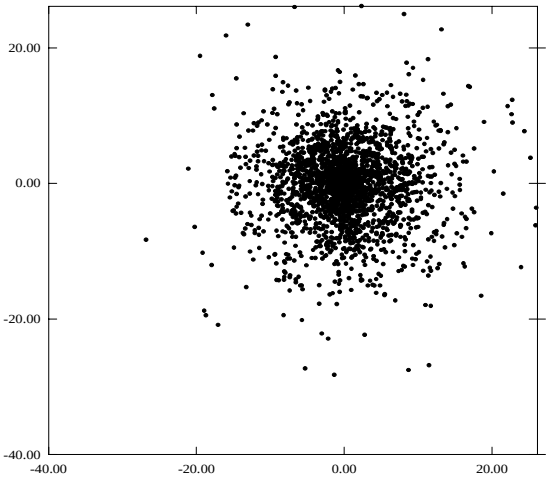

FIG.15.- The evolution of stochastic magnetic field linesin the plane (x, y) for values of (K_1, K_2)= (1.8,1.6).

C. DIFFUSION OF MAGNETIC FIELD LINES

In this paragraph, we have calculated numerically the diffusion coefficient of magnetic field lines which are described by the generalized mapping Eqts. (16). To this end, we have used expression

$$D_n = \frac{1}{2.n_p.n} \sum_{i=1}^{i=n_p} (I_n^i - I_0^i)^2 \qquad (44)$$

where n=50 is the number of iterations and n_p=3000 is the field lines number that we have considered. We have plot (Figures. 13-17) the ratio D/D_{QL} versus K_1 for different values of K_2 (K_2=0,1,5,10 and 15). The solid lines

correspond to the analytical calculation Eq. (43) while the points represent the numerical results. We see that the analytical results agree with our numerical calculations.

When K_2=0, the stochastic magnetic field lines are described by the standard mapping. In this case the ratio D/D_{QL} oscillates around the value 1 (Fig. 13). This ratio tend to 1 when K_1 increases. For K_2 is different to zero, the oscillations become more and more close to 1 when K_2 increases.

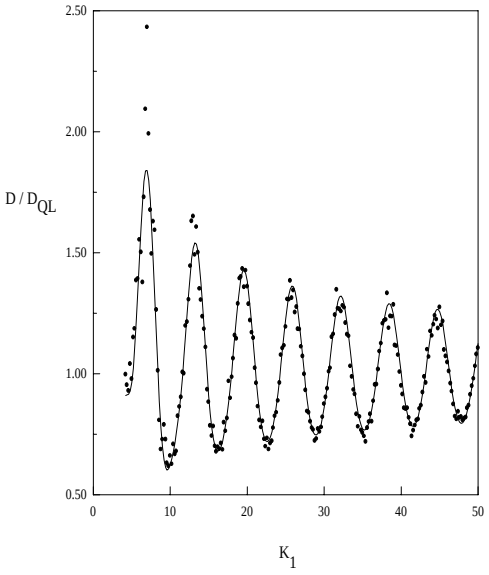

FIG. 13. Plot of the ratio D/D_{QL} versus K_1 for the mapping standard ($K_2 = 0$).

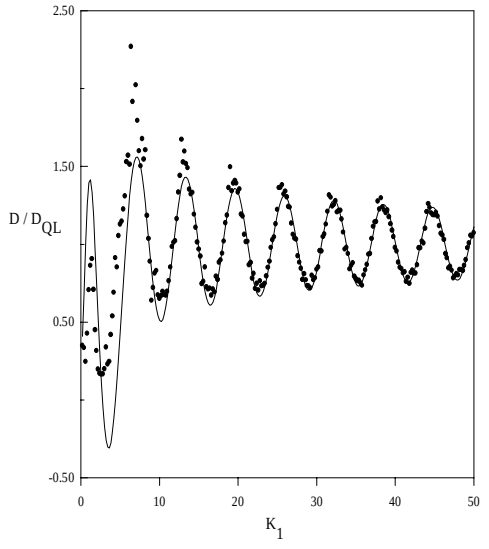

FIG. 14. Plot of the ratio D/D_{QL} versus K_1 for $K_2 = 1$.

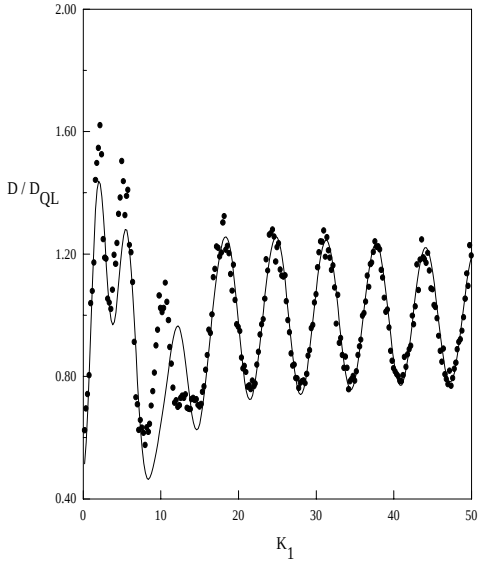

FIG. 15. Plot of the ratio D/D_{QL} versus K_1 for $K_2 = 5$.

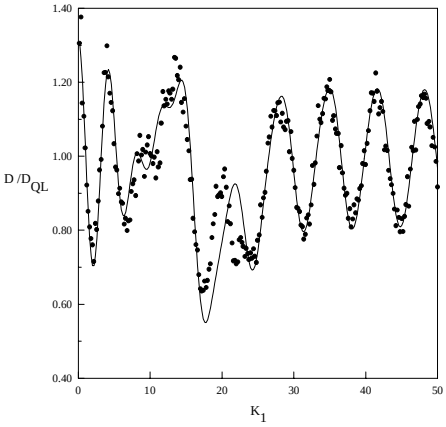

FIG. 16. Plot of the ratio D/D_{QL} versus K_1 for $K_2 = 10$.

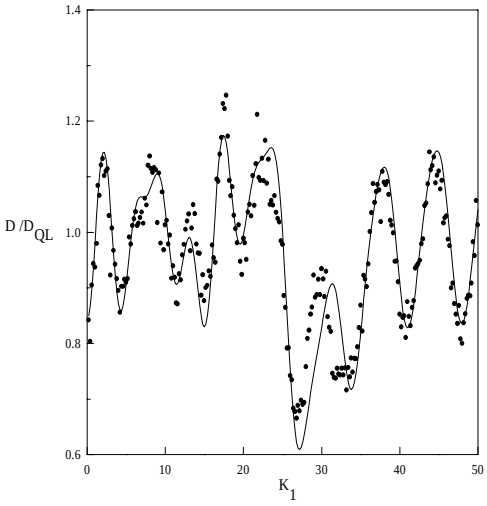

FIG. 17. Plot of the ratio D/D_{QL} versus K_1 for $K_2 = 15$.

COMMENTS OF FIELD LINES DIFFUSION

In the first part of this work, we have shown that transition from partial stochasticity to global stochasticity of magnetic field lines is produced rapidly with the generalized mapping compared to results obtained for the standard mapping.

In the second part, we have done an analytical calculation of the diffusion coefficient using the Fourier paths and the characteristic function formalism.Both methods give the same results for diffusion coefficient.

VI. CONCLUSION

It has been possible to study the anomalous transport induced by electrostatic and magnetic fluctuation. The trajectories of particle guiding centers in presence of perturbed electrostatic and magnetic field in a tokamak is showed to be described by four equations of motion.

This system can be described with Hamilton equations, using a set of action-angle variables. With only one perturbation, the trajectories are associated with an island chain in the phase space. The transition to stochasticity occurs for increasing perturbation strength between regions of the phase space. The diffusion coefficient of particles is computed and compared to the quasi-linear theory in each case. it is showed that the diffusion due to magnetic turbulence increases with the parallel velocity whereas the diffusion due to electrostatic turbulence decreases with the parallel velocity. This behavior indicate that electric fluctuations might be the dominant source of anomalous transport for the particles at low parallel velocity, whereas magnetic fluctuations effect particles transport at great velocity. A comparison between field lines diffusion and particles diffusion across magnetic surfaces shows that the field lines diffuse across the plasma and the particle motion along these field lines gives rise to the anomalous diffusion.

Bibliography:

[1] A. B. Rechester, and M. N. Rosenbluth, Phys. Rev. Lett **40**, 38 (1978)
[2] H. B. Park, E. G. Heo, W. Horton, D-I. Choi, Phy. Plasmas **4**, 3273 (1997)
[3] W. Horton, H. B. park, J-M. Kwon, D. Strozzi, P.J.Morrison, D-I. Choi, Phys. Plasmas **5**,3910 (1998)
[4] A. J. Lichtenberg, M. A. Liberman, « Regular and Stochastic Motion ». Springer Verlag, New York, 1983.
[5] F. Miskane, X.garbet, A. Dezairi and D. Saifaoui. Phys Plasmas **7**, 4197 (2000)
[6] R. Balescu, M. Vlad, F. Spineanu, in « Chaos, Kinetics and Non linear Dynamics in Fluid and Plasmas », edited by S. Benkadda and G. Zaslavsky. Springer, Berlin. 1998.
[7] A. B. Rechester, M. N. Rosenbluth, R.B. White. Phys. Rev. Lett,**42**, 1247 (1979)
[8] P. Ghendrih, A. Grosman, H. Capes. Plasma Phys. Cont. Fusion **38**, 1653 (1996)
[9] R. Tabet, D. Saifaoui, A. Dezairi, A. Rouak, European Physical Journal-Applied physics , N° **4**, 329 1998)
[10] R. Sabot, M. A. Dubois, Phys Letters A **212**, 201 (1996)
[11] R. Sabot, « importance de la structure magnétique fine dans un tokamak pour le transport anormal et les disruptions internes », thèse. Ecole Centrale de Paris, 1996.
[12] A. Oualyoudine, D. Saifaoui, A Dezairi, A. Rouak, J. Phy. **7**, 1045(1997)
[13] G. Laval, Phys. Fluids B **5**, 711, (1993)
[14]F.Miskane,A.Dezairi,D.saifaoui, H.Imzi Contribution of turbulence electrostatic and magnetic to anomalous transport in tokamak. European Physical Journal-Applied physics. Mars 2001.